Simulation-based PSHA for the Kathmandu Basin in Nepal

Rama Mohan Pokhrel
Research Associate, Dept. of Civil Engineering, University of Bristol, Bristol, UK

Raffaele De Risi
Lecturer, Dept. of Civil Engineering, University of Bristol, Bristol, UK

Maximilian J. Werner
Senior Lecturer, School of Earth Sciences, University of Bristol, Bristol, UK

Flavia De Luca
Lecturer, Dept. of Civil Engineering, University of Bristol, Bristol, UK

Paul J. Vardanega
Senior Lecturer, Dept. of Civil Engineering, University of Bristol, Bristol, UK

Prem Nath Maskey
Professor, Institute of Engineering, Tribhuvan University, Kathmandu, Nepal

Anastasios Sextos
Professor, Dept. of Civil Engineering, University of Bristol, Bristol, UK

ABSTRACT: Reliable probabilistic seismic hazard analysis (PSHA) for Nepal is a long-term goal that different researchers have been working on in the last decade. Especially after the 2015 Gorkha earthquake, several classical probabilistic seismic hazard analysis studies have been carried out for the entire Nepal. Herein, an alternative simulation-based PSHA is performed for the Kathmandu basin generating a stochastic catalogue of events using information about seismogenic zones from recent research studies. Different ground motion prediction equations have been adopted. Results show the necessity for a ground motion prediction model that is tailored for Nepal.

1. INTRODUCTION

Before the 2015 Gorkha earthquake, a number of Probabilistic Seismic Hazard Analysis (PSHA) studies for Nepal have been published (e.g., Parajuli et al. 2010; Thapa and Guoxin, 2013; Chaulagain et al. 2015) and the new evidence from the 2015 seismic events resulted in more recent studies on the topic (e.g., Ghimire and Parajuli, 2016; Subedi and Parajuli 2016; Rahman and Bai, 2018; Rout and Kamal 2018; Thapa 2014). The main challenges that emerge from examination of the literature are related to the lack of data to build a robust seismic catalogue, the uncertainties when determining the Gutenberg-Richter (GR) parameters, and the lack of Ground Motion Prediction Equations (GMPEs) for the Himalayan region. Therefore, reasonable assumptions are made such as adopting GMPEs from other parts of the world. Uncertainties are considered by means of a classic logic-tree approach (Marzocchi et al., 2015). Most of the existing studies identify seismic zones (ranging from a few to the 23 identified by Thapa and Guoxin, 2013), and for each zone GR parameters and the maximum magnitude are estimated. More recent studies used a zone-free (kernel smoothing) approach (Rout and Kamal 2018). Stevens at al. (2018) presented a detailed PSHA of Nepal with particular emphasis on the India/Eurasia subduction interface.

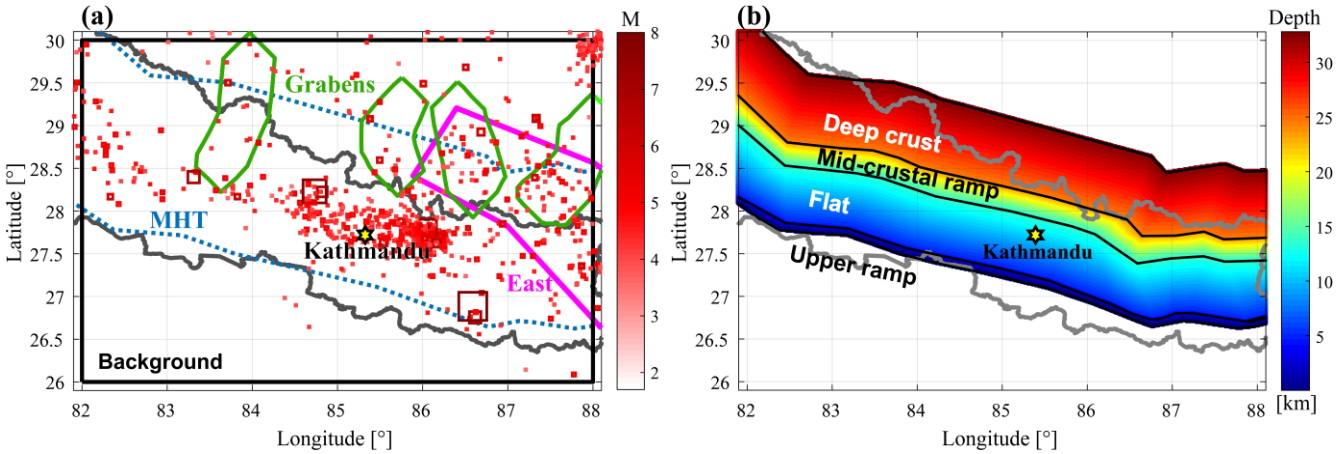

Figure 1: (a) Earthquake catalogue and seismic source zone. (b) MHT subduction plane.

They identified six seismic source zones: (1) the Main Himalayan Thrust (MHT), (2) the Karakoram fault, (3) a group of four graben zones (Northerly Grabens), (4) the Western Nepal Strike Slip and Normal Fault zone, (5) the Eastern Nepal Strike Slip Fault zone, and a (6) background seismicity zone. Building upon the work of Stevens et al. (2018), this paper presents a new simulation-based PSHA analysis for a location in Kathmandu using a bespoke Matlab code. The effect of soil amplification and the influence of different ground motion prediction models are investigated. Hazard curves for different spectral accelerations, and response spectra corresponding to a return period (T_R) of 475 years are presented. The new insights, which can be useful for the upcoming new code release in Nepal, are obtained within the framework of the project Seismic Safety and Resilience of Schools in Nepal (SAFER).

2. SEISMIC SOURCE MODELS

In this study the seismic sources presented in Stevens et al. (2018) have been considered. More specifically, only the MHT, the Northly Grabens, the Eastern region and the Background seismicity are accounted for (Figure 1a).

Only these sources have been considered since the other zones are too distant (more than 300 km) to affect the hazard in Kathmandu. The minimum magnitude considered is 5; the GR parameters calculated by Stevens et al. (2018) have been adopted (Table 1).

Table 1: GR parameters.

Zone	*a*	*b*	M_{MAX}
MHT	*6.00*	*1*	*9.2*
Eastern	*5.21*	*1*	*7.2*
Grabens	*4.87*	*1*	*7.3*
Background	*4.50*	*1*	*7.5*

2.1. MHT

To construct the geometry of the MHT the data provided by Elliott et al. (2016) have been considered together with the four zones identified by Stevens et al. (2018), namely (1) the upper ramp, ranging from the surface to about 5 km depth with a dip of 30°, (2) a nearly flat section from 5 km up to about 14 km depth with a slope of 7°, (3) the mid-crustal ramp from 14 km to about 28 km depth with a 20° slope, and (4) a flat deep crustal zone at 30 km beneath the northern Nepalese political boundary. The geometry of the MHT is presented in Figure 1b. Kathmandu is only 11 km from the nearest point on the megathrust (a small distance). In the simulation-based procedure, a uniform variability of the strike of 4° with respect to the MHT trench alignment was considered.

2.2. The Eastern Nepal Strike Slip zone

This zone is shown with the magenta line in Figure 1a. The region is dominated by deep strike slip focal mechanisms. The hypocentral depth is

assumed to span between 25 km and 50 km; the strike is assumed equal to 45° (Stevens et al. 2018). In the simulation-based procedure a uniform variability of the strike of 4° (i.e., 45° ± 2°) has been modelled.

2.3. The Northerly Grabens

This zone comprises four non-contiguous areas according to Stevens et al. (2018). Such zones, represented with the green lines in Figure 1a, are dominated by normal focal mechanisms. The hypocentral depth is assumed to span between 0 km and 20 km; the strike is assumed equal to 0° (Stevens et al. 2018). In the simulation-based procedure a uniform variability of the strike of 4° (i.e., 0° ± 2°) has been considered. Moreover, a uniform variability of the dip between 40° and 60° has been considered. Finally, the epicenter has been considered equiprobable to fall in any of the four graben areas.

2.4. Background seismicity

All other (known and unknown) seismic sources are accounted for with a background seismicity model in which any kind of earthquake can occur (i.e., normal, reverse, strike-slip) with a hypocentral depth spanning between 0 km and 75 km (Stevens et al. 2018).

3. SIMULATION-BASED PSHA FOR KATHMANDU BASIN

A simulation-based PSHA has been carried out according to Atkinson and Goda (2013) and Assatourians and Atkinson (2013). Specifically, a stochastic catalogue of earthquakes is generated according to the spatio-temporal parameters of the considered seismic sources. A Poisson earthquake occurrence model was considered. The catalogue has all the characteristics of a traditional earthquake catalogue: i.e. time, moment magnitude of the event, epicenter, but also all the characteristics of a plausible finite-fault model obtained as function of the magnitude of the events by means of scaling laws. In this work, Wells and Coppersmith (1994) scaling laws have been adopted for the crustal earthquakes and the new scaling laws proposed by Thingbaijam et al. (2017) have been adopted for the interface events. Figure 2 shows one hundred years of events generated stochastically. Having the simulated plausible finite model of the rupture is very useful as it assists with the use of ground motion prediction models that require very complex source-to-site distance definitions.

For this case study, a stochastic catalogue of 100,000 years was generated. Once the catalogue is ready, for each event, it is possible to calculate the expected intensity measure (IM) at the site by means of one or more GMPEs, considering the associated variabilities. The IMs considered herein are the Peak Ground Acceleration (PGA), and the spectral acceleration ($Sa(T_1)$) at a number of reference periods (T_1). In this preliminary work, perfect correlation between residuals at different spectral accelerations have been considered; moreover, to reduce the computational time, the scenario providing the largest yearly PGA has been adopted to calculate all the spectral accelerations. As evidenced from Figure 2, the seismicity of MHT dominates the hazard and interface events are those majorly characterising the catalogue (e.g., see the number of red fault planes in Figure 2). The percentage of interface events in the final catalogue is above the 99%.

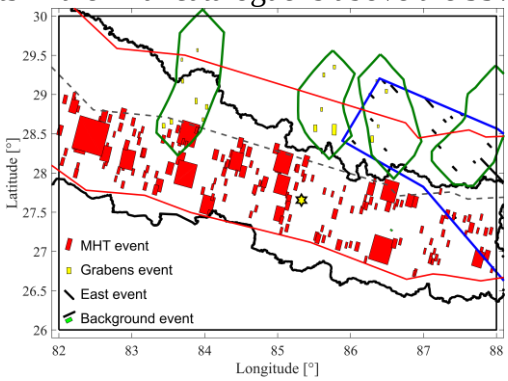

Figure 2: Twenty years of the stochastic catalogue.

3.1. Ground motion prediction equation

Given the particular seismogenic context (i.e., both subduction and crustal earthquakes), two families of GMPEs have been adopted, one for interface events and one for crustal events (Figure 3).

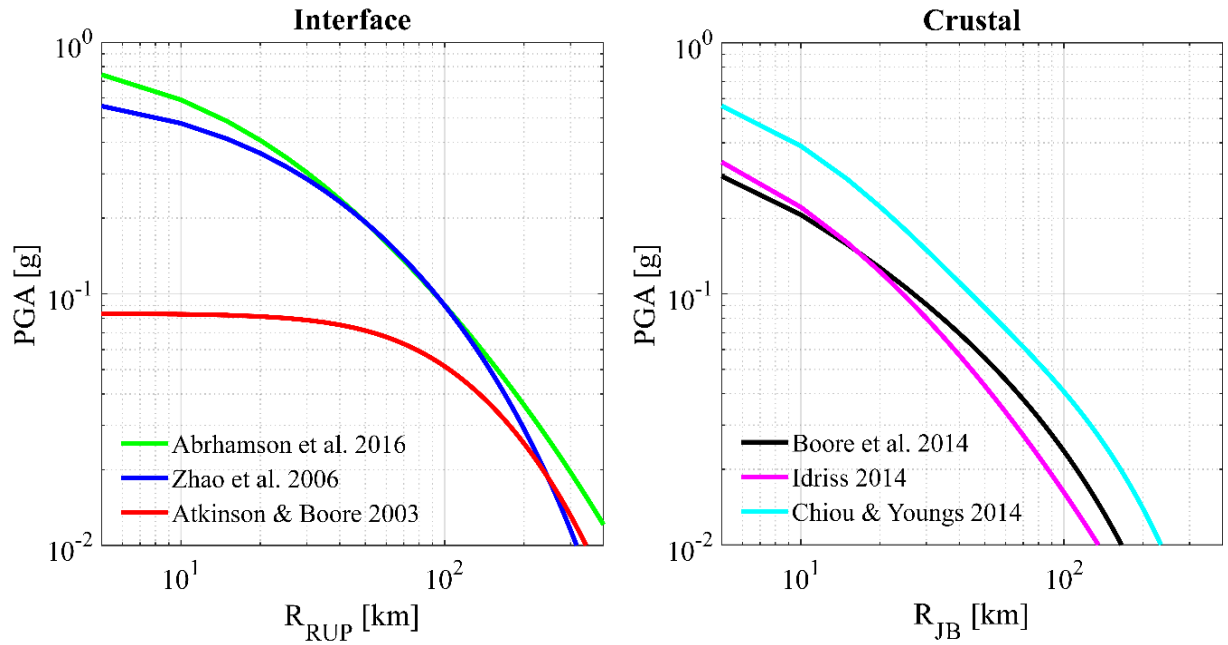

Figure 3: Mean predicted PGA at a rock site according to several GMPEs for a M_w8 interface earthquake at 15 km depth. (b) Mean predicted PGA on rock for several GMPEs for a M_w7 crustal strike-slip earthquake at 15km depth. Note the difference in the distance definition.

Specifically, for the interface events, as also suggested by Stevens at al. (2018), the GMPEs of Abrahamson et al. (2016), Zhao et al. (2006) and Atkinson and Boore (2003) have been adopted, while for crustal earthquakes, the GMPEs of Boore et al. (2014), Idriss (2014) and Chiou and Youngs (2014). All but the Idriss et al. (2014) GMPE have been used also by Stevens et al. (2018). Figure 3a shows that recent GMPEs for interface events (Abrahamson et al. 2016), as well as GMPEs based mainly on data from Japan (Zhao et al. 2006), predict substantially higher intensity measures in the near field than in the past. This effect is particularly relevant when the site of interest is only a few kilometres away from the rupture surface, as is the case for Kathmandu Valley. Figure 3b shows that the Boore et al.(2014) and the Idriss (2014) models nearly coincide and predict lower PGAs than those predicted by Chou and Youngs (2014).

In the simulations, for both crustal and interface earthquakes, the GMPEs models are considered equiprobable. Figure 3b is generated for a strike-slip mechanism to make the three GMPEs comparable as this is the only case in which the IM can be represented as a function of the same distance, i.e., the Joyner-Boore distance (R_{JB}). The Abrahamson et al. 2016 GMPE, is a model that can be used at global scale and has been herein used without the correction factor (coefficient ΔC_1) by means of which the more recent megathrust subduction events (e.g., Tohoku Japan 2011, Maule Chile 2010) can be taken into account.

3.2. Hazard curves and response spectrum

Once the IMs of interest are calculated for each event of the catalogue with the GMPEs, only the annual maximum values need to be retained to represent the hazard curves (Figure 4a). Intersecting the hazard curves obtained, corresponding to different spectral accelerations (i.e., from PGA to Sa(T=5s)), with a predefined value of probability of exceedance, it is possible to obtain the uniform hazard spectrum (UHS, Figure 4b). For the specific case of one point in the Kathmandu valley (i.e., 85.3158 longitude 27.7117 latitude, where the KATNAP station is located), the PGA on stiff soil (V_{S30} = 1000 m/s) is expected to be equal to 0.86g, and

amplifications up to a factor of 2.5 are expected for short vibration periods. This estimate excludes any site amplification and compares well with the corresponding estimate by Stevens et al. (2018) for the same point and same return period equal to ~0.65g. Stevens et al. (2018)'s PGA, however, includes the soil amplification that is based on the slope-based model by the USGS (Allen and Wald 2009) for the estimation of the average shear wave velocity in the first 30 m of soil (V_{S30}). For this point, the USGS soil model estimates a V_{S30} in the range 250 – 300 m/s. It is also interesting to observe what happens when different soil conditions are considered. To study this, four values of V_{S30} have been considered: namely, 125 m/s, 250 m/s, 500 m/s, and 1000 m/s. Figure 5a shows the four different response spectra obtained for the four different soil conditions. The anchorage PGAs for the different soil conditions are all roughly equal to 1.00g having a significantly higher value with respect to the 0.65g estimation from Stevens et al. (2018). Significant amplification can occur between 0.3 and 2.5 seconds. In this preliminary study, the formulations provided by the adopted GMPEs have been adopted for the assessment of the amplified spectral accelerations. A better uniform approach for the soil amplification may be needed, especially considering the geological and soil context of the Kathmandu basin for which the conventional V_{S30} does not necessarily provide an accurate level of information (e.g., Gilder et al. 2018).

3.3. Influence of the GMPE models

In addition to the combination of GMPEs presented above (in the following referred as GMPE Option 1), further investigation on how the UHS is affected by the GMPEs' assumptions is discussed herein.

Two additional options are studied. Option 2 consists in including the effects of recent megathrust events in the Abrahamson et al. GMPE, (i.e., $\Delta C_1 \neq 0$) and in substituting the Zhao et al. (2006) GMPE with the more recent Zhao et al. (2016) GMPE calibrated from/for Japanese events.

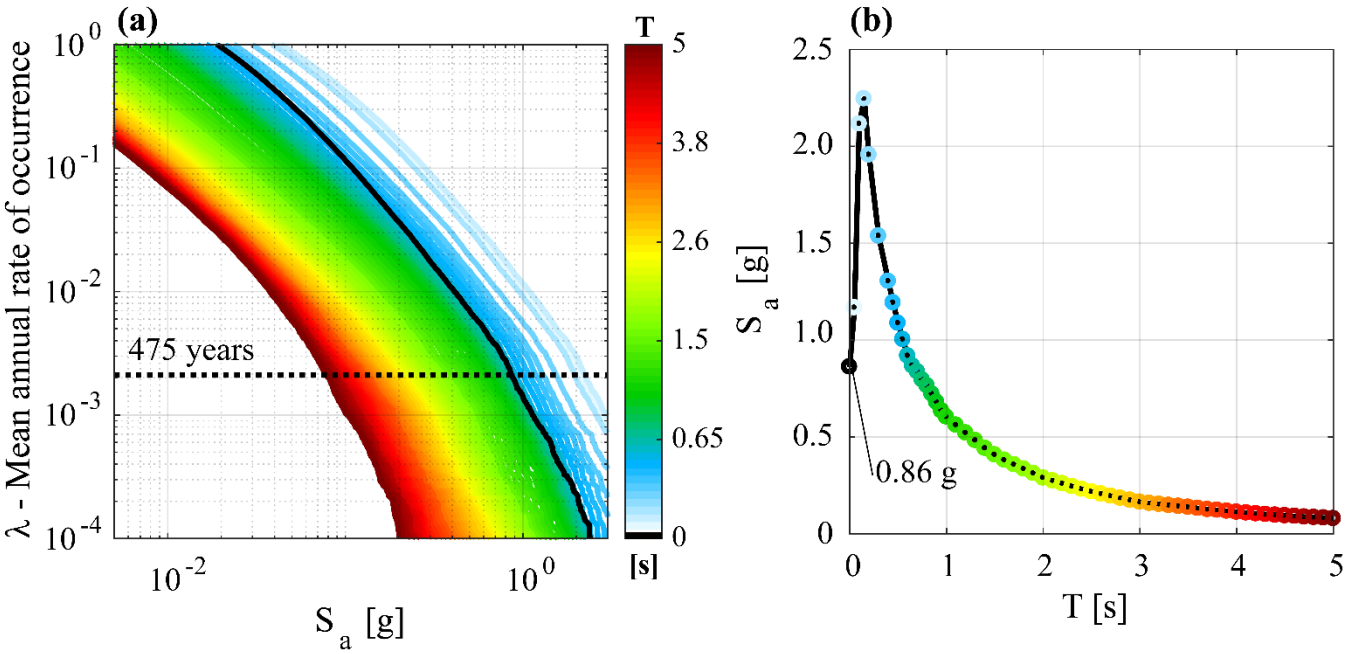

Figure 4: (a) Hazard curves for several spectra accelerations. (b) Uniform hazard spectrum corresponding for a return period of 475 years.

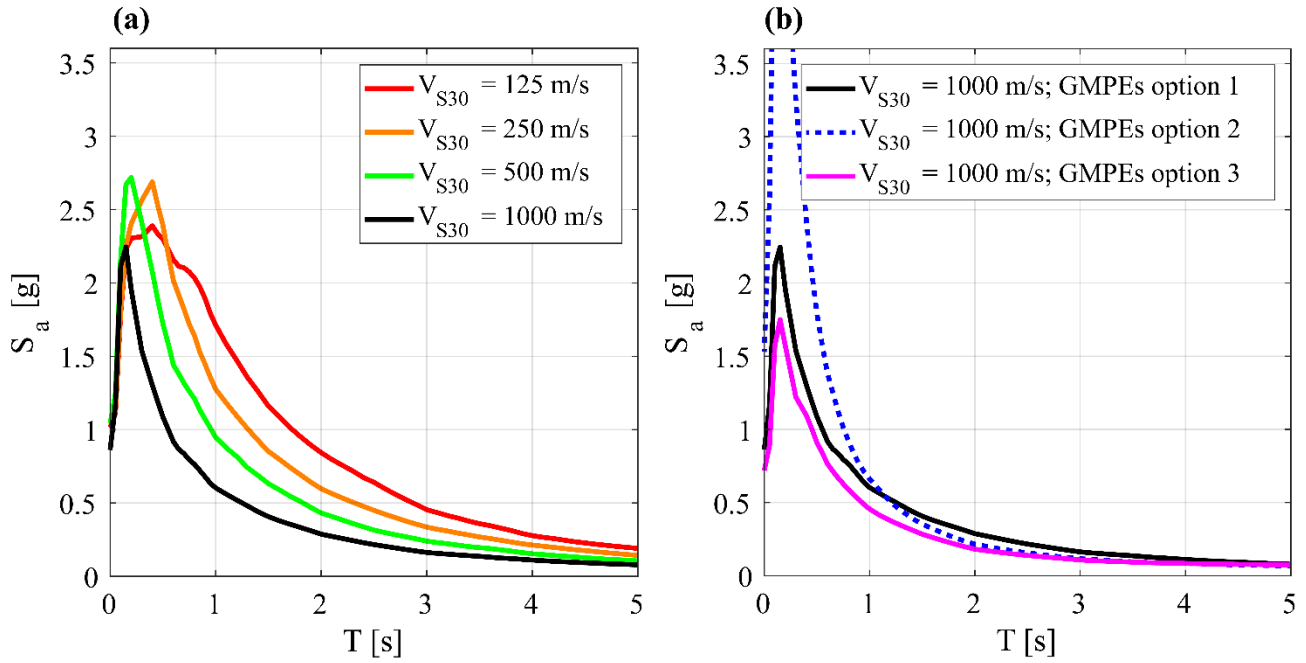

Figure 5: (a) Response spectra for different values of shear wave velocity. (b) Uniform hazard spectra for different choices of GMPEs.

Option 3 is defined as Option 1 (i.e., ΔC_1=0 in Abrahamson et al.) but disregarding the Zhao et al. (2006) GMPE. This option neglects the contribution to the final hazard of the strong Japanese interface earthquakes.

PGA values for Option 1, 2 and 3 are respectively equal to 0.86g, 1.5g and 0.72g. Figure 5b compares the three UHS corresponding to a return period of 475 years for the three aforementioned options. The assumptions in the GMPE model affect the hazard assessment at the site dramatically.

Several PSHA studies have been carried out before and after the 2015 Gorkha event. Table 2 shows the PGA values for Kathmandu according to different literature studies.

Most of the older studies provide PGA values corresponding to 475 years return period smaller than the those obtained by more recent studies. This is because the older studies consider a segmentation of the MHT in Main Boundary Thrust (MBT), Main Central Thrust (MCT), and Himalayan Frontal Thrust (HFT), considering impossible a full rupture along the subduction plane and assuming a maximum magnitude equal to 8 (i.e. for the Nepal Bihar earthquake which occurred in 1934).

Table 2: Comparison of PGA estimates for soft sediments in Kathmandu Valley (475-years T_R)

Authors	*PGA (g)*
Parajuli et al., (2010)	*0.51*
Thapa and Guoxin (2013)	*0.525*
Chaulagain et al., (2015)	*0.38*
Ghimire and Parajuli (2016)	*0.61*
Subedi and Parajuli (2016)	*0.51*
Rahman and Bai., (2018)	*0.55*
Stevens et al., (2018)	*0.65*
This study	*0.72 **

**Evaluated for V_{S30}=1000m/s and option 3*

4. CONCLUSIONS

This paper presented new insights into the probabilistic seismic hazard of Kathmandu that are very useful for the upcoming new building code release in Nepal.

A simulation-based PSHA has been developed, employing an in-house Matlab-code, for the Kathmandu basin by generating a stochastic catalogue of events from the spatial-temporal

properties of the four seismic zones described in the recent study by Stevens et al. (2018).

Hazard curves for PGA and a number of spectral accelerations are obtained for a site on rock. Also, the uniform hazard spectrum for a return period of 475 years has been obtained for a single point in the Kathmandu valley. Spectral amplification up to 2.5 times can be observed for low values of the vibration period.

Using the conventional amplification factors used by the GMPEs, the effect of soil amplification has also been investigated. Large spectral amplification can occur up to vibration period of 2.5 second.

Only 100,000 years have been simulated and the sensitivity to the length of the catalogue has not been investigated, therefore an additional effort is required with respect to this aspect; so, results should be still considered as preliminary. Moreover, with respect to previous studies (e.g., Stevens et al. 2018), GMPEs for interface and crustal events are used exclusively for such specific events.

Further discussion is needed on the applicability limitations of the adopted GMPE models (e.g., interval of Magnitude and distance).

Finally, the influence of different GMPEs on the uniform hazard spectrum has been investigated. From this preliminary study, it emerged that the influence is dramatic and potentially bespoke GMPE models for the Himalayan seismogenic context are required. This was also emphasized by Sharma et al. (2009) and is worthy of discussion since all the strong subduction earthquakes are due to the subduction of an oceanic plate under a continental one. In the case of Himalaya, there are two continental plates.

ACKNOWLEDGEMENTS

This work was funded by the Engineering and Physical Science Research Council (EPSRC) under the project “Seismic Safety and Resilience of Schools in Nepal” SAFER (EP/P028926/1).

REFERENCES

Abrahamson, N., Gregor, N., & Addo, K. (2016). BC Hydro ground motion prediction equations for subduction earthquakes. Earthquake Spectra, 32(1), 23-44.

Allen, T. I., & Wald, D. J. (2009). On the use of high-resolution topographic data as a proxy for seismic site conditions (VS 30). Bulletin of the Seismological Society of America, 99(2A), 935-943.

Assatourians, K., & Atkinson, G. M. (2013). EqHaz: An open-source probabilistic seismic-hazard code based on the Monte Carlo simulation approach. Seismological Research Letters, 84(3), 516-524.

Atkinson, G. M., & Boore, D. M. (2003). Empirical ground-motion relations for subduction-zone earthquakes and their application to Cascadia and other regions. Bulletin of the Seismological Society of America, 93(4), 1703-1729.

Atkinson, G. M., & Goda, K. (2013). Probabilistic seismic hazard analysis of civil infrastructure. In Handbook of Seismic Risk Analysis and Management of Civil Infrastructure Systems (pp. 3-28).

Boore, D. M., Stewart, J. P., Seyhan, E., & Atkinson, G. M. (2014). NGA-West2 equations for predicting PGA, PGV, and 5% damped PSA for shallow crustal earthquakes. Earthquake Spectra, 30(3), 1057-1085.

Chaulagain, H., Rodrigues, H., Silva, V., Spacone, E., & Varum, H. (2015). Seismic risk assessment and hazard mapping in Nepal. Natural Hazards, 78(1), 583-602.

Chiou, B. S. J., & Youngs, R. R. (2014). Update of the Chiou and Youngs NGA model for the average horizontal component of peak ground motion and response spectra. Earthquake Spectra, 30(3), 1117-1153.

Elliott, J.R., Jolivet, R., González, P.J., Avouac, J.P., Hollingsworth, J., Searle, M.P., & Stevens, V.L. (2016). Himalayan megathrust geometry and relation to topography revealed by the Gorkha earthquake. Nature Geoscience, 9(2), 174.

Ghimire, S., & Parajuli, H.R. (2016). Probabilistic seismic hazard analysis of Nepal

considering uniform density model. In Proceedings of IOE Graduate Conference (pp. 115-122).

Gilder, C, De Risi, R, De Luca, F, Vardanega, P, Holcombe, EA, Ayoubi, P, Asimaki, D, Mohan Pokhrel, R & Sextos, A 2018, Optimising resolution and improvement strategies for emerging geodatabases in developing countries. in Proceedings of the 16th European Conference on Earthquake Engineering., 10743, European Association for Earthquake Engineering (EAEE), 16th European Conference on Earthquake Engineering, Thessaloniki, Greece, 18-21 June.

Idriss, I. M. (2014). An NGA-West2 empirical model for estimating the horizontal spectral values generated by shallow crustal earthquakes. Earthquake Spectra, 30(3), 1155-1177.

Marzocchi, W., Taroni, M., & Selva, J. (2015). Accounting for epistemic uncertainty in PSHA: Logic tree and ensemble modeling. Bulletin of the Seismological Society of America, 105(4), 2151-2159.

Parajuli, H. R., Kiyono, J., Taniguchi, H., Toki, K., & Maskey, P.N. (2010). Probabilistic seismic hazard assessment for Nepal. WIT Transactions on Information and Communication Technologies, 43, 405-416.

Rahman, M.M., & Bai, L. (2018). Probabilistic seismic hazard assessment of Nepal using multiple seismic source models. Earth and Planetary Physics, 2(4), 327-341.

Rout, M.M., & Kamal, D.J. (2018) Probabilistic seismic hazard for Himalayan region using kernel estimation method (zone-free method). Natural Hazards, 93(2), 967-985.

Sharma, M. L., Douglas, J., Bungum, H., & Kotadia, J. (2009). Ground-motion prediction equations based on data from the Himalayan and Zagros regions. Journal of Earthquake Engineering, 13(8), 1191-1210.

Stevens, V.L., Shrestha, S.N., & Maharjan, D.K. (2018). Probabilistic Seismic Hazard Assessment of Nepal. Bulletin of the Seismological Society of America, 108 (6): 3488-3510.

Subedi, B., & Parajuli, H.R. (2016). Probabilistic seismic hazard analysis of Nepal. In Proceedings of IOE Graduate Conference (pp. 265-270).

Thapa, D.R. (2014). Seismic zoning for Nepal (Doctoral dissertation). Dalian University of Technology, China.

Thapa, D.R. and Guoxin, W (2013). Probablistic seismic hazard analysis in Nepal. Earthquake Engineering and Engineering Vibration, 12: 577-586.

Thingbaijam, K. K. S., Martin Mai, P., & Goda, K. (2017). New Empirical Earthquake Source-Scaling Laws. Bulletin of the Seismological Society of America, 107(5), 2225-2246.

Wells, D. L., & Coppersmith, K. J. (1994). New empirical relationships among magnitude, rupture length, rupture width, rupture area, and surface displacement. Bulletin of the seismological Society of America, 84(4), 974-1002.

Zhao, J. X., Zhang, J., Asano, A., Ohno, Y., Oouchi, T., Takahashi, T., ... & Fukushima, Y. (2006). Attenuation relations of strong ground motion in Japan using site classification based on predominant period. Bulletin of the Seismological Society of America, 96(3), 898-913.

Zhao, J. X., Liang, X., Jiang, F., Xing, H., Zhu, M., Hou, R., ... & Fukushima, Y. (2016). Ground-motion prediction equations for subduction interface earthquakes in Japan using site class and simple geometric attenuation functions. *Bulletin of the Seismological Society of America*, *106*(4), 1518-1534.